

The Assessment of Glioblastoma Metabolic Activity via ^{11}C -Methionine PET and Radiomics

Gleb DANILOV^{a,1}, Diana KALAEVA^b, Nina VIKHROVA^b, Tatiana KONAKOVA^b,
Anna ZAGORODNOVA^a, Angelina POPOVA^a, Andrey POSTNOV^b,
Svetlana SHUGAY^b, Michael SHIFRIN^a and Igor PRONIN^b

^aLaboratory of Biomedical Informatics and Artificial Intelligence, National Medical Research Center for Neurosurgery named after N.N. Burdenko, Moscow, Russian Federation

^bNeuroimaging Department, National Medical Research Center for Neurosurgery named after N.N. Burdenko, Moscow, Russian Federation

^cNational Research Nuclear University MEPhI, Moscow, Russian Federation

^dLebedev Physical Institute of the Russian Academy of Science, Moscow, Russian Federation

^eJSC Research Institute of Technical Physics and Automation, Moscow, Russian Federation

ORCID ID: Gleb Danilov <https://orcid.org/0000-0003-1442-5993>

Abstract. Nowadays, the quantitative analysis of PET/CT data in patients with glioblastoma is not strictly standardized in the clinic and does not exclude the human factor. This study aimed to evaluate the relationship between the radiomic features of glioblastoma ^{11}C -methionine PET images and the tumor-to-normal brain (T/N) ratio determined by radiologists in clinical routine. PET/CT data were obtained for 40 patients (mean age 55 ± 12 years; 77.5% men) with a histologically confirmed diagnosis of glioblastoma. Radiomic features were calculated for the whole brain and tumor-containing regions of interest using the RIA package for R. We redesigned the original RIA functions for GLCM and GLRLM calculation to reduce computation time significantly. Machine learning over radiomic features was applied to predict T/N with the best median correlation between the true and predicted values of 0.73 ($p = 0.01$). The present study showed a reproducible linear relationship between ^{11}C -methionine PET radiomic features and a T/N indicator routinely assessed in brain tumors. Radiomics enabled utilizing texture properties of PET/CT neuroimaging that may reflect the biological activity of glioblastoma and can potentially augment the radiological assessment.

Keywords. Glioblastoma, radiomics, neuroradiomics, PET, machine learning, artificial intelligence, neurosurgery

¹ Corresponding author: Gleb Danilov, N.N. Burdenko Neurosurgery Center, 4th Tverskaya-Yamskaya str. 16, Moscow 125047, Russian Federation; E-mail: glebda@yandex.ru.

1. Introduction

Glioblastoma is the most common primary malignant astrocytic neoplasm of the brain [1]. A valuable neuroimaging modality in glioblastoma diagnostics is PET/CT with radiopharmaceutical. The intensity of its uptake in a tumor relative to a normal brain (tumor-to-normal brain ratio, T/N) correlates with the biological aggression of the neoplasm. To date, the quantitative analysis of PET/CT data in patients with glioblastoma is not strictly standardized in the clinic and does not exclude the human factor. Radiomics can promote unification and increase the objectivity and informativeness of neuroimaging assessment [2]. This study aimed to evaluate the relationship between the radiomic features of glioblastoma ^{11}C -methionine PET images and the T/N ratio determined by radiologists in clinical routine. We believe the proposed approach facilitates the standardization and automation of radiological biomarkers production in clinical practice.

2. Methods

Our observational study was conducted under the ethical principles in the Helsinki Declaration of the World Medical Association (1964). We obtained PET images from adult patients with supratentorial glioblastoma treated at the National Medical Research Center for Neurosurgery named after N.N. Burdenko between 2018 and 2020. To assess the relative metabolic activity of ^{11}C -methionine in glioblastoma by PET as a clinical routine, the average values of the standardized uptake value (SUV) were calculated in 1.0 cm^3 of the most active tumor region (SUV_t) and 1.0 cm^3 of normal brain tissue of the contralateral frontal lobe (SUV_n). Then the tumor-to-brain ratio was derived as $T/N = \text{SUV}_t/\text{SUV}_n$.

To calculate the radiomic features, MRI and PET/CT were co-registered using the PMOD software (v 4.0). Voxel values outside of the head contours were eliminated. A fixed-size rectangular area of interest was set for all the co-registered slices to capture the maximum tumor volume on any level. Thus, in a 3D space, the entire tumor was enclosed in a parallelepiped. Then, for each patient, the whole 3D array of PET voxels (“whole brain” dataset, WBD) and a subset of the 3D array of PET voxels in a given parallelepiped (“cropped brain” dataset, CBD) were exported to separate NIFTI files, which were used to compute radiomic features.

Calculations and data analysis were performed using the R programming language (version 4.2.2) in the RStudio Server IDE (version 2022.07.0+548) on an NVIDIA DGX A100 supercomputer. Radiomic features were computed from PET 3D array using the *RIA* library [3]. The voxel values from CBD were discretized into 2, 4, 8, 16, 32, 64, and 128 bins. WBD was discretized only into 128 levels to reduce the time and computation burden. We calculated first-order, gray level co-occurrence matrix (*GLCM*), gray level run length matrix (*GLRLM*) and geometry-based statistics (the complete list of features is presented in [4]). To compute PET radiomic features for the entire 3D brain image, we redesigned the original functions from the *RIA* package that calculate *GLCM* and *GLRLM*. That accelerated the computations a thousandfold and enabled the whole brain radiomics with a reasonable amount of time.

At the first step of data analysis, we selected radiomic features showing statistically significant Pearson correlation with the T/N ratio ($p < 0.05$). Then the linear regression models with LASSO regularization were trained over selected radiomics features as

predictors and T/N ratio as the target variable using *glmnet* library. The predictors were normalized, and the target variable was transformed using the decimal logarithm. Machine learning was repeated in 300 tests. The training and test samples were randomly split in each trial as 70% and 30% of the original dataset. The mean absolute error (MAE), root mean squared error (RMSE), and Pearson and Spearman correlation coefficients between the true and predicted T/N values were calculated in each test to evaluate prediction quality. The results from all tests were summarized to produce more robust estimates.

3. Results

A total of 40 independent preoperative PET/CT studies from 40 patients (31 (77.5%) men and 9 (22.5%) women, avg. age 55 ± 12 years) were included. The median T/N ratio obtained by neuroradiologists for PET studies was 3.26 [2.74; 4.17], and the minimum and maximum values were 1.94 and 5.03. MAE, RMSE, and the number of predictors (NoP) in models summarized from 300 tests as median [25% quantile; 75% quantile] and calculated exclusively on test samples, as well as the minimum (Min NoP) and the maximum (Max NoP) number of predictors, are presented in Table 1. The numbers in dataset names (“2_4..._128” or “_128”) denote all discretization levels for images from which the radiomics parameters included in the dataset were calculated.

Table 1. The quality metrics of linear regression models summarized from 300 tests for various sets of radiomic features.

Dataset	MAE	RMSE	NoP	Min NoP	Max NoP
WBD_128_CBD_128	0.49 [0.41;0.58]	0.68 [0.54;0.85]	14 [11;16]	4	32
WBD_128_CBD_2_4_8_16_32_64_128	0.52 [0.45;0.63]	0.75 [0.62;0.91]	17 [14;20]	2	37
CBD_128	0.54 [0.46;0.64]	0.76 [0.63;0.94]	9 [7;12]	1	27
CBD_2_4_8_16_32_64_128	0.56 [0.47;0.67]	0.61 [0.45;0.74]	11 [9;15]	1	28
WBD_128	0.72 [0.63;0.81]	0.90 [0.79;1.02]	9 [6;12]	0	23

Table 2 shows the correlation between the predicted and true T/N ratio for linear regression models with regularization and its statistical significance calculated on test samples and presented as median [25% quantile; 75% quantile]. The rows in Tables 1 and 2 range from best (top) to worst (bottom) performance.

Table 2. Correlation between the predicted and true T/N ratios.

Dataset	Correlation	Coefficient	P-value
WBD_128_&_CBD_128	Pearson	0.71 [0.55;0.82]	0.01 [0.00;0.06]
WBD_128_&_CBD_128	Spearman	0.73 [0.55;0.81]	0.01 [0.00;0.07]
WBD_128_&_CBD_2_4_8_16_32_64_128	Pearson	0.67 [0.53;0.77]	0.02 [0.00;0.08]
WBD_128_&_CBD_2_4_8_16_32_64_128	Spearman	0.67 [0.51;0.80]	0.02 [0.00;0.09]
CBD_128	Pearson	0.64 [0.45;0.80]	0.03 [0.00;0.14]
CBD_128	Spearman	0.67 [0.48;0.80]	0.02 [0.00;0.12]
CBD_2_4_8_16_32_64_128	Pearson	0.61 [0.45;0.74]	0.03 [0.01;0.14]

CBD_2_4_8_16_32_64_128	Spearman	0.62 [0.47;0.78]	0.04 [0.00;0.12]
WBD_128	Pearson	0.36 [0.20;0.53]	0.24 [0.08;0.49]
WBD_128	Spearman	0.42 [0.28;0.56]	0.17 [0.06;0.38]

Figures 1A and 1C show the regression lines between true and predicted T/N ratios superimposed for 300 tests over WBD_128_CBD_128 dataset (best performance) and WBD_128 dataset (worst performance), respectively. Similarly, figures 1B and 1D present the locally weighted scatterplot smoothing (LOESS) lines for all the tests to catch the most common trends.

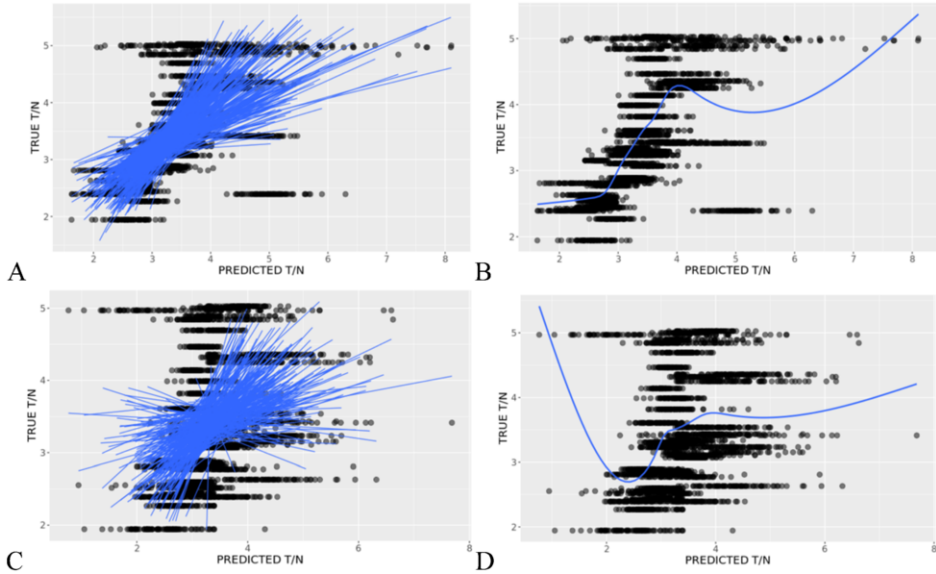


Figure 1. The scatterplot of predicted vs. true T/N ratios from 300 tests. A – superimposed regression lines, WBD_128_CBD_128 dataset; B – LOESS line, WBD_128_CBD_128 dataset; C – superimposed regression lines, WBD_128 dataset; B – LOESS line, WBD_128 dataset;

4. Discussion

The present study showed a reproducible linear relationship between ^{11}C -methionine PET radiomic features and a T/N indicator routinely assessed for brain tumors. In other words, we demonstrated the fundamental capability of calculating radiomics-based complex PET biomarkers that could be clinically relevant, e.g. as predictors of tumor proliferative activity. It is essential that these regularities were found for glioblastoma PET images - within one top-malignant histological tumor type. However, these effects should be tested within a comprehensive histological range.

The impact of whole brain radiomics is well-noted in Tables 1 and 2 and Figures 1. The WBD alone is less effective compared to sole CBD in predicting T/N. The combination of radiomic features from a set of cropped images with different discretization levels is slightly inferior to CBD with one top-discretization level. However, combining radiomic features from the entire brain and its tumor-containing area provided the best value. That strikes the importance of selecting the regions of

interest for radiomics (not limited to the visible tumor) and the possible effect of discretization, which should be further tested.

A common radiomics application in glioblastoma imaging studies is the differential diagnosis, overall survival prognosis, and molecular biomarkers prediction [5]. However, radiomics was rarely used to study PET/CT glioblastoma images [6]. The potential clinical significance of radiological PET biomarkers was previously shown in survival research for patients with glioblastoma [7]. The application of radiomics to ^{11}C -methionine PET is extremely rare. To the best of our knowledge, this is the first study to combine local and whole-brain radiomics to predict tumor metabolic activity by PET/CT with ^{11}C -methionine.

The main limitations of our study are the small sample size and the lack of standards for identifying the local region of interest in capturing the tumor. Our future work will address more radiomic features evaluation on larger samples.

Conclusion

Radiomics enables utilizing texture properties of PET/CT neuroimaging that may reflect the biological activity of glioblastoma and can potentially augment the radiological assessment. Despite the current limitations in the application, the first results indicate the promising potential of neuroradiomics. The regularities found in this research should be tested with a larger amount of data.

The study was supported by the Ministry of Science and Higher Education of the Russian Federation under agreement No. 075-15-2021-1343.

References

- [1] Ostrom QT, Cioffi G, Waite K, Kruchko C, Barnholtz-Sloan JS. CBTRUS statistical report: primary brain and other central nervous system tumors diagnosed in the United States in 2014–2018. *Neuro-oncology*. 2021 Oct;23(Supplement_3):iii1-05.. doi:10.1093/NEUONC/NOAB200.
- [2] Litvin AA, Burkin DA, Kropinov AA, Paramzin FN. Radiomics and digital image texture analysis in oncology. *Современные технологии в медицине*. 2021;13(2 (eng)):97-104. doi:10.17691/STM2021.13.2.11.
- [3] RIA package manual, (n.d.). <https://cran.r-project.org/web/packages/RIA/vignettes/RIA.html> (accessed November 25, 2022).
- [4] Kolosváry M, Karády J, Szilveszter B, Kitslaar P, Hoffmann U, Merkely B, Maurovich-Horvat P. Radiomic features are superior to conventional quantitative computed tomographic metrics to identify coronary plaques with napkin-ring sign. *Circulation: Cardiovascular Imaging*. 2017 Dec;10(12):e006843..
- [5] Zhu M, Li S, Kuang Y, Hill VB, Heimberger AB, Zhai L, Zhai S. Artificial intelligence in the radiomic analysis of glioblastomas: A review, taxonomy, and perspective. *Frontiers in Oncology*. 2022;3793. doi:10.3389/FONC.2022.924245.
- [6] Martin P, Holloway L, Metcalfe P, Koh ES, Brighi C. Challenges in Glioblastoma Radiomics and the Path to Clinical Implementation. *Cancers*. 2022 Aug 12;14(16):3897. doi:10.3390/CANCERS14163897.
- [7] Li Z, Holzgreve A, Unterrainer LM, Ruf VC, Quach S, Bartos LM, Suchorska B, Niyazi M, Wenter V, Herms J, Bartenstein P. Combination of pre-treatment dynamic [18F] FET PET radiomics and conventional clinical parameters for the survival stratification in patients with IDH-wildtype glioblastoma. *European Journal of Nuclear Medicine and Molecular Imaging*. 2023 Jan;50(2):535-45. doi:10.1007/S00259-022-05988-2/TABLES/3.